Available online at www.sciencedirect.com
ScienceDirect
European Journal of Medicinal Chemistry 43 (2008) 1376–1389
EUROPEAN JOURNAL OF MEDICINAL CHEMISTRY
http://www.elsevier.com/locate/ejmech

Original article

Antitumor studies – Part 2: Structure–activity relationship study for flavin analogs including investigations on their in vitro antitumor assay and docking simulation into protein tyrosine kinase

Hamed I. Ali [a], Keiichiro Tomita [a], Eiichi Akaho [b,*], Munetaka Kunishima [b], Yutaka Kawashima [c], Takehiro Yamagishi [c], Hisao Ikeya [c], Tomohisa Nagamatsu [a,**]

[a] *Division of Pharmaceutical Sciences, Graduate School of Medicine, Dentistry and Pharmaceutical Sciences, Okayama University, 1-1-1 Tsushima-naka, Okayama 700-8530, Japan*
[b] *Faculty of Pharmaceutical Sciences, Life Science Center, Kobe Gakuin University, 1-1-3 Minatojima, Chuo-ku, Kobe, Hyogo 650-0045, Japan*
[c] *Medicinal Research Laboratories, Taisho Pharmaceutical Co., Ltd, 1-403 Yoshino-cho, Ohmiya-shi, Saitama 303-8530, Japan*

Received 14 June 2007; received in revised form 25 September 2007; accepted 4 October 2007
Available online 14 October 2007

Abstract

Various analogs of flavins, 5-deazaflavins, and flavin-5-oxides were docked into the binding site of protein tyrosine kinase $pp60^{c\text{-}src}$, and some of them were assayed for their potential antitumor and PKC (protein kinase C) inhibitory activities in vitro. The results considering SAR (structure–activity relationship) revealed that the higher binding affinities obtained include compounds with the structure modifications on the flavin or 5-deazaflavin skeleton, namely, NH_2 or Ph (phenyl-) group at the C-2 position and so on. Computationally designed compounds **4a**, **6a**, **b**, **7**, **11b**, **c**, **12**, **15**, and **22c** exhibited good docking results suggesting that they are potentially active antitumor agents. These compounds have 1–3 phenyl moieties, which are thought to be responsible for the planar aromatic fitting or electrostatic attraction onto the groove of the binding pocket.

Keywords: Protein tyrosine kinase; Flavin analog; AutoDock; SAR (structure–activity relationship)

1. Introduction

A series of flavin analogs have been previously developed in our group as potential antiproliferative agents in vitro [1–4], some of which (e.g. 2-deoxo-2-phenyl-5-deazaflavins and flavin-5-oxides) have exhibited antitumor activity against different tumor cell lines (NCI-H 460, HCT 116, A 431, CCRF-HSB-2, and KB) comparable or moderately superior to cisplatin. Because we are also interested in structure-based rational design of the above-mentioned flavin analogs, the elucidation of mechanism for their action is crucial for further structure improvements in order to develop more potent antitumor compounds. In the preliminary mechanistic study, we revealed that 5-deazaflavins and 2-deoxo-2-phenyl-5-deazaflavins act as selective inhibitor of protein kinase C (PKC) and exhibited effective growth inhibition against cancer cell lines such as A 431 and HT 1080 cells [1]. Protein tyrosine kinases (PTK) are attractive targets for the design of novel therapeutic agents not only against cancer but also against many other diseases [5]. Consequently, selective inhibitors of protein tyrosine kinases have attracted significant interest for the development of potential anti-neoplastic agents [6]. Computer docking technique plays an important role in the drug design as well as in the mechanistic study by placing a molecule into the binding site of the target macromolecule in a non-covalent

Abbreviations: PKC, protein kinase C; SAR, structure–activity relationship; Ph, phenyl-; PTK, protein tyrosine kinase; RMSD, root mean square deviation.

* Corresponding author. Tel.: +81 78 974 4765; fax: +81 78 974 5689.
** Corresponding author. Tel.: +81 86 251 7931; fax: +81 86 251 7926.
E-mail addresses: akaho@pharm.kobegakuin.ac.jp (E. Akaho), nagamatsu@pheasant.pharm.okayama-u.ac.jp (T. Nagamatsu).

0223-5234/$ - see front matter © 2007 Elsevier Masson SAS. All rights reserved.
doi:10.1016/j.ejmech.2007.10.011

fashion [7]. DOCK [8] and AutoDock [9] as flexible docking programs enable us to predict favorable protein–ligand complex structures with a reasonable accuracy and speed. These docking programs, when used prior to experimental screening, can be considered as powerful computational filters to reduce labor and cost needed for the development of potent medicinal compounds. AutoDock is said to offer a reasonable result in comparison with other popular docking programs [10]. The docking technique will undoubtedly continue to play an important role in drug discovery [11]. Several drugs that were designed by intensive use of computational methods are currently under investigation for clinical trials [12].

Actually, 5-deazaflavins have attracted great interest because 5-deazaflavins were the first compounds synthesized as flavin antagonists [13]. The 10-aryl-5-deazaflavin derivatives were preliminarily reported to act as inhibitors of E 3 of HMD 2 in tumors that retain wild-type P 53 [14]. Some 5-amino-5-deazaflavin derivatives also revealed potential activity towards L 1210 and KB tumor cells [15]. However, a challenging problem remains for the design of an appropriate in vivo model to evaluate the antitumor efficacy of many non-cytotoxic PTK inhibitors [16].

In this study, we verified the binding capabilities of these compounds to the PTK using a novel in silico approach. The objective of this study is to investigate structure–activity relationships (SARs) of different compounds including 5-deazaflavins [2,3,17–19], 5-deazaalloxazines [20–22], 10-alkylated-2-deoxo-5-deazaflavins [4,19,23,24], 5-amino-5-deaza flavin derivatives [15], 10-alkylated-2-deoxoflavin-5-oxides [4], 2-methyl, 2-methylthio, 2-piperidino, and 2-(*N*-hydroxymethyl-*N*-methyl) derivatives of 2-deoxo-5-deazaflavins [23], 2-deoxo-2-phenylalloxazines [25], vertical- and horizontal-type bispyridodipyrimidines [26,27], and computationally designed 2-deoxoflavins, pyridodipyrimidines, and pyrimidopteridines. In this study, the investigated compounds include 58 synthetically known compounds, of which 37 compounds [4,15,17,19,24] revealed potential antitumor and tyrosine kinase inhibitory activities. Herein, we report the PKC inhibitory activities and the antiproliferative potency of these molecules against KB tumor cells in addition to their docking mode into the binding site of PTK pp60$^{c\text{-}src}$ (pdb code: 1skj). Moreover, a series of computations were performed to predict their binding mode and their binding affinities, and for the investigation of their structural features, which revealed the highest fitting within PTK so as to help us design potent PTK inhibitors.

2. Results and discussion

2.1. In vitro PKC inhibitory activity and antiproliferative potency of flavin analog against KB tumor cells

The biological activities of the synthetically known compounds of various 5-deazaflavins and flavin-5-oxides (Scheme 1) have not yet been well determined. Therefore, we herein prepared those compounds to study their biological activities. Generally speaking, 5-deazaflavins {pyrimido[4,5-*b*]quinoline-2,4(3*H*,10*H*)-diones} (**1**), [2,3,17–19] 10-substituted or unsubstituted 2-deoxo-5-deazaflavins (**2**),[4,19] and 5-deazaalloxazine {pyrimido[4,5-*b*]quinoline-2,4(1*H*,3*H*)-dione} (**3**) [20–22] were synthesized by condensation of *o*-halogenobenzaldehydes and 6-*N*-alkyl- or 6-*N*-aryl-aminouracil, or by Vilsmeier–Haack reaction of 6-anilinouracils or 6-anilinopyrimidin-4(1*H*)-ones. These compounds were identified with the authentic samples by their IR and ^{1}H NMR spectra. 5-Deazaflavin derivatives (**1a–l**) and 2-deoxo-5-deazaflavins (**2a–d**, **j**) were tested for their in vitro PKC inhibitory activities and antiproliferative effect against human oral epidermoid carcinoma cell line (KB) using H-7 [1-(5-isoquinolinylsulfonyl)-2-methylpiperazine] and Ara-C as positive controls, respectively. Compounds **1d**, **2a**, **b**, **d**, and **j** showed good PKC inhibition of 10.0, 3.54, 12.9, 4.55, and 14.8 μg/mL (IC_{50}), respectively. Other compounds **1a**, **e–g**, **i–k** exhibited reasonable PKC inhibition of *ca*. 24–90 μg/mL (IC_{50}). Regarding the activity against KB tumor cells, 5-deazaflavins (**1a–l**) are inactive, while 2-deoxo-2-phenyl-5-deazaflavins (**2a–d**, **j**) exhibited the IC_{50} of 0.67, 0.79, 2.53, 1.17 and 17.9 μg/mL, respectively, as shown in Table 1.

Automated docking studies were carried out using AutoDock version 3.05 [9]. The three different search algorithms offered by AutoDock 3.05, including Monte Carlo simulated annealing (SA), Lamarckian genetic algorithm (GA), and genetic algorithm with local search (GALS). The preliminary trial runs were carried out and we found that GALS was the most efficient, reliable, and successful search algorithm. Therefore, it was selected to model the interaction/binding between PTK pp60$^{c\text{-}src}$ and flavin analogs. It showed good correlation between the IC_{50} against PKC for the potentially active compounds, i.e. **1a**, **e–g**, **i–k** and **2a**, **b**, **d**, **j**, and we obtained their estimated AutoDock binding free energies (ΔG_b) with the correlation coefficient (R^2) value of 0.593 as shown in Fig. 1. This figure was plotted based on our intention that it should include all compounds investigated so as to avoid bias or unfair comparison. It is our understanding that the positive correlation coefficient (R^2) values, especially 0.5 or above, plotting biological activity of compounds and their docking binding free energies, are regarded as reasonable [26]. In this figure, compounds **1e**, **g**, and **2d** appear to be somewhat out of the model. This discrepancy is to show the limitation of comparison between the two systems due to the fact that there are lots of unsolved areas such as inclusion of the protein movement into the computational system, incorporation of such scoring functions as atomic elasticity of the compounds, atomic vibration and rotation of the compounds and so on.

The structure–activity relationship (SAR) was studied by alternation of different structural moieties of 5-deazaflavins (**1a–s**) [2,3,17–19], 2-deoxo-5-deazaflavins (**2a–v**) [4,19,23,24], 5-deazaalloxazine (**3a–c**) [20–22], 7,10-dimethyl-2-deoxo-2-phenylflavin-5-oxide (**6c**) [4], 2-deoxo-2-phenylalloxazines (**9a**) [25], 5-alkylamino-5-deazaflavins (**10c–l**) [15], vertical- and horizontal-type bispyridodipyrimidines (**16** and **17a**, **b**) [27,28], and the computationally designed 2-deoxo-5-deazaalloxazines (**4a–r**), 3-phenylalloxazines (**5a–k**), 2-deoxo-2-phenylflavin-5-oxide (**6a**, **b**), 3,10-diphenylflavin-5-oxide (**7**), 2-deoxo-7,

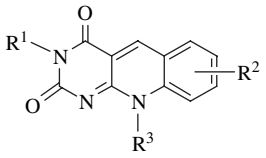

1a–s

a: $R^1 = R^2 = H$, R^3 = *n*-Bu
b: $R^1 = H$, R^2 = 8-Cl, R^3 = *n*-$C_{12}H_{25}$
c: $R^1 = R^2 = H$, R^3 = Ph
d: $R^1 = H$, R^2 = 7-Me, R^3 = Et
e: R^1 = Me, $R^2 = H$, R^3 = Et
f: R^1 = Me, $R^2 = H$, R^3 = *n*-Pr
g: R^1 = Me, $R^2 = H$, R^3 = *n*-Bu
h: R^1 = Me, $R^2 = H$, R^3 = Ph
i: R^1 = Me, R^2 = 7-Me, R^3 = Ph
j: R^1 = Ph, $R^2 = H$, R^3 = Me
k: R^1 = Ph, $R^2 = H$, R^3 = Et
l: $R^1 = R^3$ = Ph, $R^2 = H$
m: $R^1 = R^2 = H$, R^3 = Me
n: $R^1 = R^2 = H$, R^3 = Et
o: $R^1 = R^2 = H$, R^3 = *n*-Pr
p: $R^1 = R^2 = H$, R^3 = *i*-Pr
q: $R^1 = R^2 = H$, R^3 = 4-Cl-C_6H_4
r: $R^1 = R^2 = H$, R^3 = 4-Me-C_6H_4
s: $R^1 = R^2 = H$, R^3 = 3,4-Me_2-C_6H_3

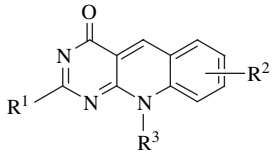

2a–v

a: R^1 = Ph, $R^2 = H$, R^3 = Me
b: R^1 = Ph, $R^2 = H$, R^3 = Et
c: R^1 = Ph, $R^2 = H$, R^3 = *n*-Bu
d: R^1 = Ph, R^2 = 7-Me, R^3 = Me
e: R^1 = Ph, R^2 = 6,7,8-$(OMe)_3$, R^3 = Me
f: R^1 = Ph, $R^2 = R^3 = H$
g: R^1 = Ph, R^2 = 9-Me, $R^3 = H$
h: R^1 = Ph, R^2 = 8-OMe, $R^3 = H$
i: R^1 = Ph, $R^2 = H$, R^3 = Ph
j: $R^1 = NH_2$, $R^2 = H$, R^3 = Me
k: $R^1 = NH_2$, $R^2 = R^3 = H$
l: $R^1 = NH_2$, R^2 = 7-Me, $R^3 = H$
m: $R^1 = NH_2$, R^2 = 7-OMe, $R^3 = H$
n: $R^1 = NH_2$, R^2 = 8-OMe, $R^3 = H$
o: $R^1 = NH_2$, $R^2 = H$, R^3 = Ph
p: R^1 = SMe, $R^2 = R^3 = H$
q: R^1 = SMe, $R^2 = H$, R^3 = Ph
r: R^1 = Me, $R^2 = R^3 = H$
s: R^1 = Me, $R^2 = H$, R^3 = Ph
t: R^1 = piperidino, $R^2 = H$, R^3 = Ph
u: R^1 = piperidino, $R^2 = R^3 = H$
v: $R^1 = N(CH_2CH_2OH)Me$, $R^2 = H$, R^3 = Ph

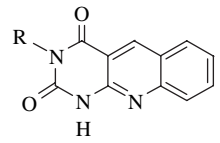

3a–c

a: R= H
b: R = Me
c: R = Ph

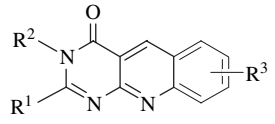

4a–r

a: R^1 = Ph, $R^2 = R^3 = H$
b: R^1 = Ph, $R^2 = H$, R^3 = 7-Me
c: R^1 = Ph, $R^2 = H$, R^3 = 7-OMe
d: R^1 = Ph, $R^2 = H$, R^3= 7-Cl
e: R^1 = Ph, $R^2 = H$, R^3 = 7-OH
f: R^1 = Ph, $R^2 = H$, R^3 = 8-Me
g: R^1 = Ph, $R^2 = H$, R^3 = 9-Me
h: R^1 = Ph, $R^2 = H$, R^3= 8-Cl
i: R^1 = Ph, $R^2 = H$, R^3 = 8-OH
j: R^1= Ph, $R^2 = H$, R^3 = 8-OMe
k: R^1 = Ph, $R^2 = H$, R^3 = 6,7,8-$(OMe)_3$
l: R^1 = Ph, $R^2 = H$, R^3 = 7-COOH
m: R^1 = Ph, R^2 = Me, R^3= H
n: $R^1 = NH_2$, $R^2 = R^3 = H$
o: $R^1 = NH_2$, $R^2 = H$, R^3 = 7-Me
p: $R^1 = NH_2$, $R^2 = H$, R^3 = 7-OMe
q: $R^1 = NH_2$, R^2 = Me, $R^3 = H$
r: $R^1 = NH_2$, R^2 = Ph, $R^3 = H$

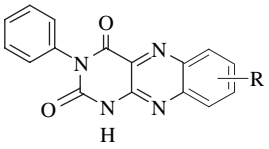

5a–k

a: R = H
b: R = 7-Me
c: R = 7-OMe
d: R = 7-Cl
e: R = 7-OH
f: R = 8-Me
g: R = 9-Me
h: R = 8-Cl
i: R = 8-OH
j: R = 8-OMe
k: R = 6,7,8-$(OMe)_3$

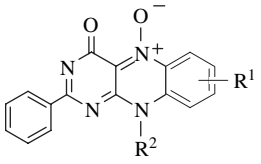

6a–c

a: $R^1 = R^2 = H$
b: R^1= 7-Cl, $R^2 = H$
c: R^1 = 7-Me, R^2 = Me

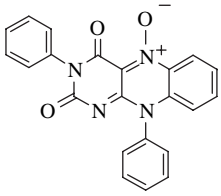

7

Scheme 1. Structures of 5-deazaflavins (**1**), 2-deoxo-5-deazaflavins (**2**), 5-deazaalloxazines (**3**), 2-deoxo-5-deazaalloxazines (**4**), 3-phenylalloxazines (**5**), 2-deoxo-2-phenylflavin-5-oxides (**6**), and 3,10-diphenylflavin-5-oxide (**7**).

Table 1
In vitro IC_{50} of 5-deazaflavins (**1a**–**l**) and 2-deoxo-5-deazaflavins (**2a**–**d**, **j**) against PKC and KB cells and their AutoDock binding free energies (ΔG_b) docked into PTK

Compound	PKC IC_{50} (μg/mL)	KB IC_{50} (μg/mL)	ΔG_b (kcal/mol)
1a	89.7	>10	+1.00
1b	>100	>10	−0.30
1c	>100	>10	−7.20
1d	10.0	>10	+0.39
1e	46.6	>10	+0.44
1f	46.0	>10	−0.45
1g	23.9	>10	+0.04
1h	>100	>10	−4.48
1i	26.4	>10	−2.21
1j	60.1	>10	−0.12
1k	53.3	>10	−1.09
1l	>100	>10	−7.02
2a	3.54	0.67	−4.67
2b	12.9	0.79	−2.50
2c	ND	2.53	−0.84
2d	4.55	1.17	−1.44
2j	14.8	17.9	−3.71
H-7[a]	38.4	ND	ND
Ara-C	ND	0.14	ND

ND: not determined.
[a] 1-(5-Isoquinolinylsulfonyl)-2-methylpiperazine.

10-dimethyl-2-phenylflavin (**8**), 2-deoxo-2-phenylalloxazine-7-carboxylic acid (**9b**), pyridodipyrimidines (**11a**–**c**, **12**, **13a**–**f**, **14**, and **15**), and pyrimidopteridines (**18a**, **b**, **19**, **20**, **21**, and **22a**–**c**) as represented in Schemes 1 and 2. These computationally designed compounds were modeled upon the structures cited in literatures [25,29,30] and will be synthesized facilely after their docking investigations.

2.2. Validation of the docking performance and accuracy

In the latest version of AutoDock 3.05 based on the traditional molecular force-field model of interaction energy, a new scoring function at the level of binding free energy was derived and adopted [9]. The most straightforward method for validation of the scoring function is to inspect how closely the best-scored docked conformation resembles the bound ligand in the experimental crystal structure. As cited in literature [11], if the RMSD (root mean square deviation) value of the best-scored conformation is ≤2.0 Å from the experimental one, the prediction is said to be successful. Therefore, validation of the accuracy of AutoDock 3.05 was done by docking of the native ur2 ligand {4-[3-carboxymethyl-3-(4-phosphonooxybenzyl)ureido]-4-[(3-cyclohexylpropyl)-methylcarbamoyl]butyric acid} of PTK $pp60^{c\text{-}src}$ (pdb code: 1skj) into its binding site [31]. The obtained success rates of AutoDock were excellent as shown in Fig. 2. The RMSD values for the top three conformations were 0.59 Å (which is shown in Fig. 2), 0.81 and 0.56 Å. It is clearly noticed that the docked ligand was exactly superimposed on the intact one of high binding affinity (ΔG_b: −10.09 kcal/mol). Moreover, the docked ligand exhibited five true hydrogen bonds with Arg 32 (N_1H), Arg 32 (N_2H), Ser 34(OH), Glu 35(NH), and His 58(O), which were exactly the same amino acids as those involved in the crystallized bound ligand. These docking results indicated the high accuracy of the AutoDock 3.05 in comparison with the biologically bounded crystal structure [31].

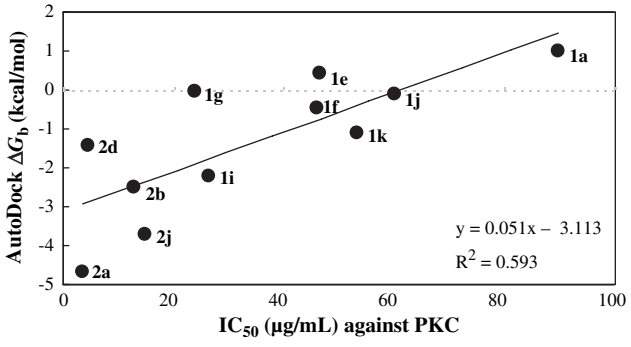

Fig. 1. Correlation between the binding free energy (ΔG_b) and IC_{50} (μg/mL) of 5-deazaflavin analogs (**1a**, **e**–**g**, **i**–**k** and **2a**, **b**, **d**, **j**) against PKC.

2.3. Docking investigation for C-2 substitution of 5-deazaflavins and 5-deazaalloxazines

In general, 2-deoxo-5-deazaflavins (**2**) with Ph or NH_2 substituent at the C-2 position exhibited lower binding docking energies into the binding site of PTK $pp60^{c\text{-}src}$. As shown in Table 2, compounds **2i**, **k**–**o** exhibited lower binding energies being ΔG_b from −7.77 to −5.86 kcal/mol. Also 2-deoxo-5-deazaalloxazines (**4a**, ΔG_b: −8.03 kcal/mol) fitted properly into the binding site. Their higher affinities are mainly attributed to hydrogen bond formation between the amino acids of the target site and 2-amino groups of the docked inhibitors. As shown in Fig. 3, 2-amino-2-deoxo-5-deazaflavin (**2k**, ΔG_b: −6.62 kcal/mol) and 2-amino-2-deoxo-7-methoxy-5-deazaalloxazine (**4p**, ΔG_b: −6.92 kcal/mol) fitted properly into the groove of the binding site. Their C-2-amino groups are located between amino acids Arg 12 and Glu 35, where 4–5 hydrogen bonds are shown between amino acids of the target site (Arg 12, Arg 32, and Glu 35) and their C_2-amino and C_4-oxo groups. Also van der Waals interaction of the C-2-phenyl moiety enhances this fitting. On the other hand, compounds with methylthio, methyl, piperidino, and 2-(*N*-hydroxyethyl-*N*-methylamino) substituents at the C-2 position such as **2p**–**v** showed less potential affinity than the above cited analogs, because they have a high binding energy (ΔG_b: from −4.35 to −2.45 kcal/mol) into the target site. These derivatives are unable to form any hydrogen bond within the target site and cannot interact with van der Waals surface.

2.4. Docking investigation for N-3 substitution of 5-deazaflavins and 5-deazaalloxazines

The 5-deazaflavin analogs with no substituent (**1c**, **3a**, and **4a**) and with a phenyl group (**1l**, **3c**, and **4r**) at the 3-position exhibited enhanced docking affinities with lower binding energies (ΔG_b). This is obviously shown for 5-deazaflavins

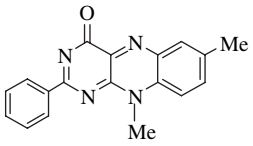

8

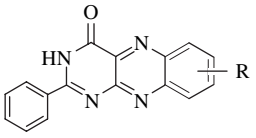

9a, b

a: R= H
b: R = 7-COOH

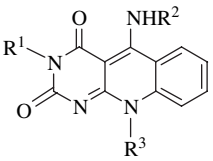

10a–l

a: R^1 = H, R^2 = H, R^3 = Me
b: R^1 = H, R^2 = Me, R^3 = Me
c: R^1 = H, R^2 = phenethyl, R^3 = Ph
d: R^1 = H, R^2 = *n*-octyl, R^3 = Ph
e: R^1 = Me, R^2 = phenethyl, R^3 = Et
f: R^1 = Me, R^2 =*n*-octyl, R^3 = Et
g:R^1 = Me, R^2 = phenethyl, R^3 = Bu
h: R^1 = Me, R^2 =*n*-octyl, R^3 = Bu
i: R^1 = Me, R^2 = phenethyl, R^3 = *n*-octyl
j: R^1= Me, R^2 = R^3 = *n*-octyl
k: R^1 = Me, R^2 = phenethyl, R^3 = *n*-dodecyl
l: R^1 = Me, R^2 = *n*-octyl, R^3 = *n*-dodecyl

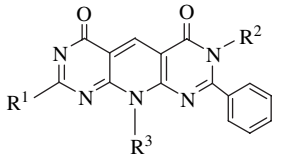

11a–c

a: R^1 = R^2= R^3 = Ph
b: R^1 = NH_2, R^2 = Ph, R^3 = H
c: R^1 = Ph, R^2 = R^3 = H

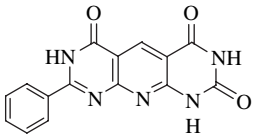

12

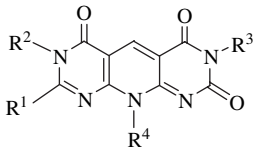

13a–f

a: R^1 = R^2 = R^3 = Ph, R^4 = Me
b: R^1 = R^2 = Ph, R^3 = H, R^4 = Me
c: R^1 = NH_2, R^2 = R^3 = H, R^4 = Ph
d: R^1 = NH_2, R^2= Me, R^3= H, R^4 = Ph
e: R^1 = NH_2, R^2= R^4 = Me, R^3 = Ph
f: R^1 = NH_2, R^2= R^4 = Me, R^3 = H

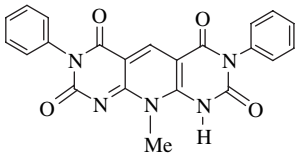

14

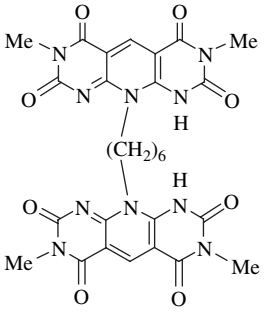

16

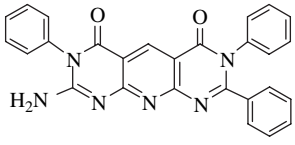

15

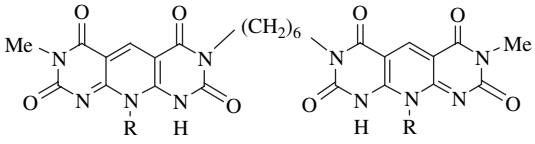

17a,b

a: R = H
b: R = Me

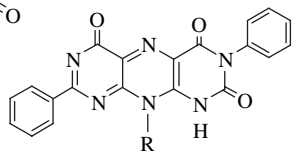

18a,b

a: R = H
b: R = Ph

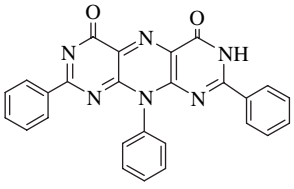

19

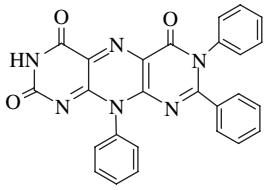

20

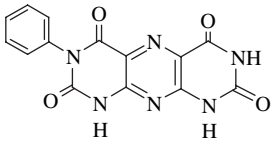

21

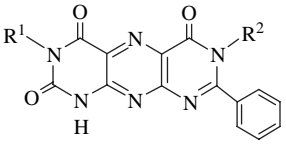

22a–c

a: R^1 = R^2 = H
b: R^1 = H, R^2 = Ph
c: R^1 = R^2 = Ph

Scheme 2. Structures of 2-deoxo-7,10-dimethyl-2-phenylflavin (**8**), 2-deoxo-2-phenylalloxazines (**9**), 5-alkylamino-5-deazaflavins (**10**), pyridodipyrimidines (**11**–**15**), bispyridodipyrimidines (**16**, **17**), and pyrimidopteridines (**18**–**22**).

(**1c**, −7.20 kcal/mol; **1l**, −7.02 kcal/mol), 5-deazaalloxazines (**3a**, −7.00 kcal/mol; **3c**, −6.88 kcal/mol), and 2-deoxo-5-deazaalloxazines (**4a**, −8.03 kcal/mol; **4r**, −6.96 kcal/mol). The *N*-3-methyl derivatives revealed higher binding energies (ΔG_b) (i.e. lower binding affinities) than those of *N*-3-H and *N*-3-Ph derivatives as shown for 5-deazaflavin (**1h**, −4.48 kcal/mol), 5-deazaalloxazine (**3b**, −4.25 kcal/mol), and 2-deoxo-5-deazaalloxazines (**4m**, −4.99 kcal/mol; **4q**, −4.97 kcal/mol). The enhanced docking affinity for *N*-3-Ph or *N*-3-H derivatives may be attributed to the bulk tolerance

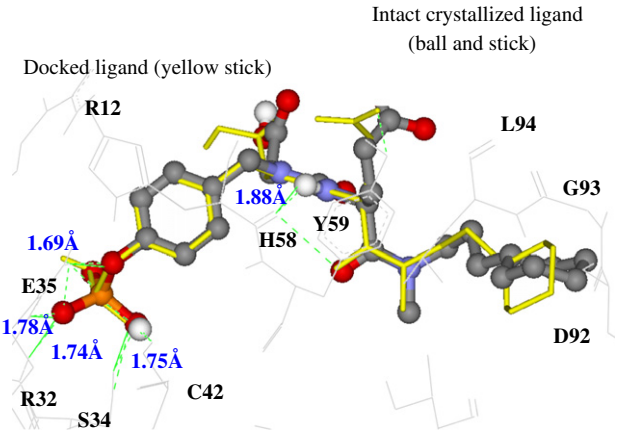

Atoms of ur2 ligand involved in hydrogen bonds.

Atom	Amino acid	Distance (Å)	Angle (°)	RMSD (Å)
HN_5	O of His (H58)	1.88	134.5	
O_2P	HO of Ser (S34)	1.75	157.5	
O_1P	HN of Glu (E35)	1.69	161.0	0.59
O_1P	HN of Arg (R32)	1.74	155.6	
O_4P	HN of Arg (R32)	1.78	142.8	

$\Delta G_b = -10.09$ kcal/mol

Fig. 2. Docking of the original ur2 ligand of PTK $pp60^{c\text{-}src}$ into its binding site. The intact crystallized ur2 ligand is shown in ball and stick, colored by element, and its hydrogen bonds are shown as green dotted lines. The docked ligand is shown in yellow stick exactly superimposed on the original one, and its hydrogen bonds are shown as green lines. (For interpretation of the references to color in the text, the reader is referred to the web version of this article.)

of *N*-3-phenyl accompanied with electrostatic surface attraction into the groove of the binding site or to the hydrogen bond formation by hydrogen at the 3-position. On the other hand, the methyl group cannot be involved in any of these interactions. The type of substituent at the C-2, N-3, and N-10 positions plays a significant role to orient the docked inhibitors into the binding site as shown in Fig. 4. The inhibitor **4a** (ΔG_b: −8.03 kcal/mol) was docked deeply and oriented horizontally in the plane of the groove of the target site, where its C-2 phenyl moiety was accommodated into the groove between Arg 12 and Glu 35 and it shows three hydrogen bonds between amino acids of Arg 32 and Glu 35. The inhibitor **1c** (ΔG_b: −7.20 kcal/mol) was embedded vertically into the pocket showing a lower binding affinity. It shows two hydrogen bonds with Ser 34 and Glu 35. Inhibitor **1l** (ΔG_b: −7.02 kcal/mol) was docked similar to **1c**, but slightly shifted away from the groove of the binding site due to its two bulky phenyl moieties at the N-3 and N-10 positions, which prevent the ligand from fitting into the binding pocket. Therefore, it shows only one hydrogen bond with His 58. In contrast, inhibitor **1a** (ΔG_b: +1.00 kcal/mol) was rejected away from the pocket. This will mainly be attributed to its N-10-bulky butyl fragment, which can be involved neither in van der Waals nor in hydrogen bond interactions, and thus leads to its improper fitting [32].

Table 2
AutoDock binding free energies (ΔG_b) and inhibition constants (K_i) for 2-deoxo-5-deazaflavins (**2i–v**) with R^1substituents altered, 5-deazalloxazines (**3a–c**), and 2-deoxo-5-deazaalloxazines (**4a**, **m–r**) docked into PTK

Compound	R^1	ΔG_b (kcal/mol)	K_i
2i	Ph	−7.77	2.01E−06
2j	NH_2	−3.71	0.00
2k	NH_2	−6.62	1.42E−05
2l	NH_2	−5.86	5.07E−05
2m	NH_2	−7.06	6.72E−06
2n	NH_2	−6.66	1.31E−05
2o	NH_2	−6.67	1.30E−05
2p	Sme	−3.50	0.00
2q	Sme	−3.92	0.00
2r	Me	−3.93	0.00
2s	Me	−4.35	6.50E−04
2t	Piperidino	−3.37	0.00
2u	Piperidino	−2.45	0.02
2v	$N(CH_2CH_2OH)Me$	−3.19	0.00
3a		−7.00	7.37E−06
3b		−4.25	7.70E−04
3c		−6.88	9.07E−06
4a	Ph	−8.03	1.29E−06
4m	Ph	−4.99	2.18E−04
4n	NH_2	−6.85	9.51E−06
4o	NH_2	−5.86	5.09E−05
4p	NH_2	−6.92	9.33E−06
4q	NH_2	−4.97	2.28E−04
4r	NH_2	−6.96	7.89E−06

2.5. Docking investigation for C and N at the 5-position of flavin ring

Docking investigation and in vitro assay revealed a successful drug-design feature of flavin-5-oxide (**6**) [4] and compound **4** which exhibited 2–5 times better affinities than those of the corresponding flavin (**8**) and 5-deazaflavin analogs (**2**). Thus, compounds **6a** and **b** considered as the best docked compounds into the binding site showed the binding energies (ΔG_b) of −7.76 and −7.67 kcal/mol and exhibited five and three hydrogen bonds, respectively. Moreover, AutoDock study revealed that flavin-5-oxide (**6c**, ΔG_b: −6.92 kcal/mol, IC_{50} against CCRF-HSB-2: 0.5 μM) [4] was docked deeply into the groove of the binding pocket of PTK forming two hydrogen bonds between Glu 35 (NH) and Ser 34 (OH) via its N_5-oxide and C_4-oxo group, respectively. On the other hand, 5-deazaflavin (**2d**, ΔG_b: −1.44 kcal/mol, IC_{50} against CCRF-HSB2: 1.49 μM) [4] was docked in the same position of its computationally designed 2-deoxoflavin isomer (**8**, ΔG_b: −2.61 kcal/mol) as shown in Fig. 3. Both **2d** and **8** did not exhibit any hydrogen bond within the binding site. It was clearly demonstrated that there was reasonable correlation between IC_{50} and binding free energy of **6c** (7,10-dimethyl-2-deoxo-2-phenylflavin-5-oxide) and **2d** (7,10-dimethyl-2-deoxo-2-phenyl-5-deazaflavin). There is also no significant difference between flavins and 5-deazaflavins regarding their docking affinities into the binding pocket as shown in Fig. 3. The fact that CH and N of the compounds are equivalent bioisosteres with similar size and comparable electronic properties may explain this phenomenon. Various 5-

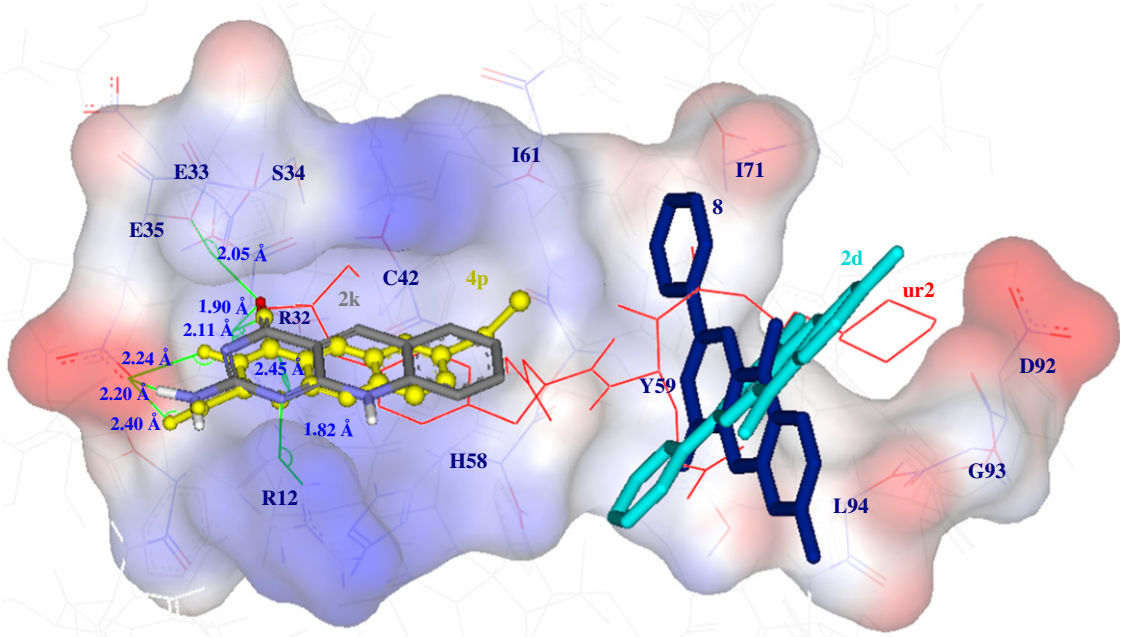

Atoms involved in hydrogen bonds

Atom of 2k	Amino acid	Distance (Å)	Angle(°)
N_1-N	HN of Arg (R12)	1.82	138.4
C_2-NH	O of Glu (E35)	2.20	134.8
C_4-Oxo	HN of Glu (E35)	2.05	158.5
C_4-Oxo	HN_1 of Arg (R32)	1.90	153.6
C_4-Oxo	HN_2 of Arg (R32)	2.45	136.8

ΔG_b= –6.62 kcal/mol; RMSD = 7.19 Å

Atoms involved in hydrogen bonds

Atom of 4p	Amino acid	Distance (Å)	Angle (°)
C_2-NH	O of Glu (E35)	2.40	123.3
N_3-H	O of Glu (E35)	2.24	144.2
C_4-Oxo	HN_1 of Arg (R32)	2.11	150.4
C_4-Oxo	HN_2 of Arg (R32)	2.21	147.7

ΔG_b = –6.92 kcal/mol; RMSD = 7.31 Å

Fig. 3. The deep docking of 2-amino-2-deoxo-5-deazaflavin (**2k**) is shown in stick, colored by element, and 2-amino-2-deoxo-7-methoxy-5-deazaallxazine (**4p**) is shown in yellow ball and stick into the groove of the binding site of PTK, whereas compound 2d, cyan stick, is docked away from the groove at the same position of its 2-deoxoflavin isomer (**8**), blue stick. The ur2 ligand is shown in red line. (For interpretation of the references to color in the text, the reader is referred to the web version of this article.)

amino-5-deazaflavin derivatives (**10c–l**) with a potential activity against L 1210 and KB tumor cells have been reported [15]. These compounds showed the following binding free energy (ΔG_b) into PTK, i.e. **10c**, +0.28 kcal/mol; **10d**, −0.14 kcal/mol; **10e**, +0.38 kcal/mol; **10f**, +0.89 kcal/mol; **10g**, +0.46 kcal/mol; **10h**, +0.72 kcal/mol; **10i**, +0.53 kcal/mol; **10j**, +0.57 kcal/mol; **10k**, +0.56 kcal/mol; **10l**, +1.18 kcal/mol. However, the overall correlation between their in vitro IC_{50} values and their binding affinities predicted by AutoDock was rather poor as can be seen from their high binding energies being in the range of −0.14 to 1.18 kcal/mol. Actually, the presence of hydrophobic substituents at R^2 and R^3 helps to explain why the ligands **10c–j** do not fit well into the pocket. In addition, the steric hindrance of the phenethyl, octyl, and dodecyl moieties interfered with their physical docking into the receptor site. The favorable docking of 5-amino analogs (**10a**, **b**) with a less bulky substituent proved this hypothesis, where they exhibited better affinities of ΔG_b: −7.23 and −6.68 kcal/mol, respectively, and with three hydrogen bonds observed for each of them. Therefore, these less bulky analogs with the higher number of hydrogen bonds, with the lowest binding energy, and with the smallest RMSD are generally expected to be a reasonable inhibitor candidate for the biological examination [32].

2.6. Docking investigation for C-7, C-8, and C-9 substitutions on the benzene ring of flavin and 5-deazaflavin structures

All analogs substituted by hydrophobic (Cl, Me and OMe) or hydrophilic (COOH and OH) substituents on the benzene ring of flavin and 5-deazaflavin structures exhibited lower affinities than those of the corresponding unsubstituted analogs as shown in Table 3. Thus, the unsubstituted 5-deazaalloxazine (**4a**, ΔG_b: −8.03 kcal/mol) and alloxazine (**5a**, ΔG_b: −7.31 kcal/mol) exhibited the lowest binding free energies. On the other hand, 2-deoxo-6,7,8-trimethoxy-2-phenyl-5-deazaalloxazine (**4k**) and 3-phenyl-6,7,8-trimethoxyalloxazine (**5k**) exhibited higher ΔG_b of −2.54 and −2.48 kcal/mol, respectively. This low affinity is due to the steric hindrance of substituents on the aryl ring, which interfere with their surface interaction and the planar fitting of the aryl moiety into the pocket of PTK. However, the compounds substituted by 7-OH (**4e**, −7.45 kcal/mol; **5e**, −6.55 kcal/mol)

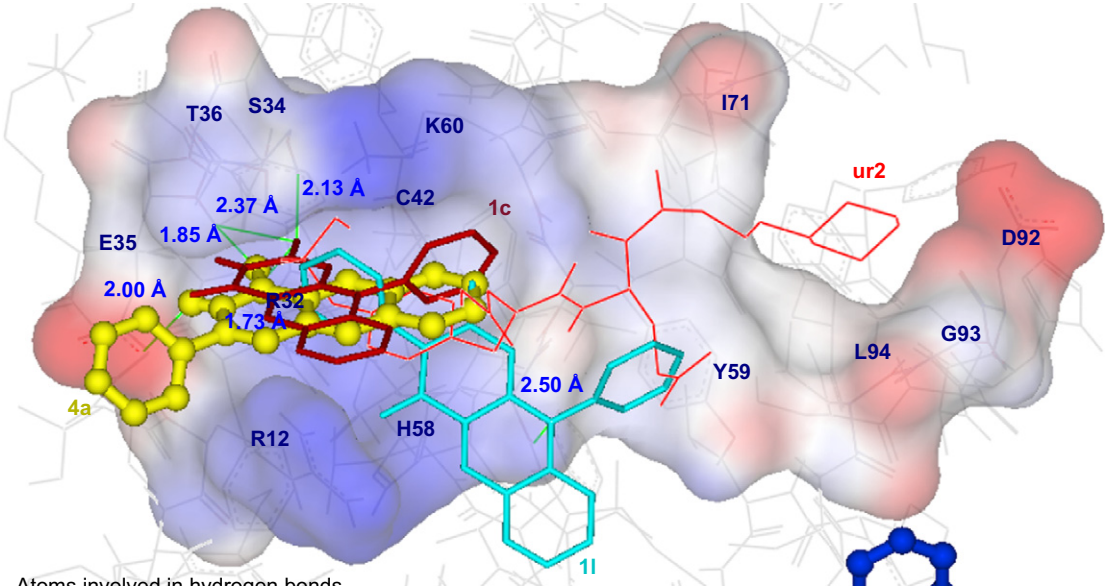

Atoms involved in hydrogen bonds.

	Atom	Amino acid	Distance (Å)	Angle (°)	ΔG_b (kcal/mol)	RMSD (Å)
4a	N_3-H	O of Glu (E35)	2.00	126.9	–8.03	8.35
	C_4-Oxo	HN of Arg (R32)	1.73	120.6		
	C_4-Oxo	HN of Glu (E35)	1.85	136.9		
1c	C_2-Oxo	HO of Ser (S34)	2.13	147.8	–7.20	6.62
	C_2-Oxo	HN of Glu (E35)	2.37	136.6		
1l	N_{10}-N	HN of His (H58)	2.50	159.3	–7.02	3.77
1a	—	—	—	—	1.00	15.49

Fig. 4. Inhibitor **4a** (yellow, ball and stick) is docked horizontally to the plane of the groove of the binding site of PTK, where its C-2 phenyl moiety is accommodated between Arg 12 and Glu 35, while **1c** (red, stick) is embedded perpendicularly into the groove. Compound **1l** (cyan, stick) is slightly shifted away from the pocket, and **1a** (blue, ball and stick) is rejected from the pocket. The binding pocket is shown in solid surface and the ur2 ligand is shown in red lines. (For interpretation of the references to color in the text, the reader is referred to the web version of this article.)

or 8-OH (**4i**, −7.36 kcal/mol; **5i**, −6.76 kcal/mol) exhibited comparatively good binding affinities, because, such hydroxyl moiety is involved in creating more hydrogen bonds, compared with other hydrophobic substituents. As shown in Fig. 5, the hydroxyl group of compound (**4e**) is involved in forming four hydrogen bonds with OH of Ser 34, NH of Glu 35, and NH and OH of Thr 36 and exhibited ΔG_b being −7.45 kcal/mol, whereas its 6,7,8-trimethoxy analog (**4k**) was poorly embedded into the target site exhibiting ΔG_b being −2.54 kcal/mol without any hydrogen bond due to its trisubstituents.

2.7. Docking investigation for N-10 substitution of 5-deazaflavin analogs

Phenyl substitution at the N-10 position of the 5-deazaflavin was favorable for the binding affinity into PTK as shown in the binding free energies (ΔG_b), e.g. **1c** (−7.20 kcal/mol), **1l** (−7.02 kcal/mol), **2i** (−7.77 kcal/mol), and **2o** (−6.67 kcal/mol), whereas the lower binding affinities of derivatives with *N*-10-Ph and *N*-3-Me such as **1h** (−4.48 kcal/mol) and **1i** (−2.21 kcal/mol) were revealed. Also, the alkyl or halogen substituted on the *N*-10-phenyl moiety exhibit less binding affinity (i.e. slightly higher binding energy, ΔG_b) such as **1q** (−4.77 kcal/mol), **1r** (−4.73 kcal/mol), and **1s** (−3.96 kcal/mol). This can be explained by the improper fitting of these compounds into the binding site due to their bulkiness. Also the N-10 substitution with alkyl group exhibited an ascending increase of the binding free energy with the increase of the carbon chain of the homologous series as shown for 5-deazaflavin derivatives, namely, **1m** (−3.75 kcal/mol, *N*-10-Me), **1n** (−1.21 kcal/mol, *N*-10-Et), **1o** (−0.86 kcal/mol, *N*-10-*n*-Pr), **1p** (+0.38 kcal/mol, *N*-10-*i*-Pr), **1a** (+1.00 kcal/mol, *N*-10-*n*-Bu), and **1b** (+1.40 kcal/mol, *N*-10-*n*-$C_{12}H_{25}$). The same effect was also shown in 2-deoxo-2-phenyl-5-deazaflavins **2a** (−4.67 kcal/mol, *N*-10-Me), **2b** (−2.50 kcal/mol, *N*-10-Et), and **2c** (−0.84 kcal/mol, *N*-10-*n*-Bu). This emphasizes the negative effect of the *N*-10-alkyl substitution on the binding affinity.

2.8. Docking investigation for isosteric replacement of phenyl ring by pyrimidine-4-one

Replacement of pyrimidoquinoline ring of 5-deazaflavins or benzopteridine ring of flavins by pyridodipyrimidines or

Table 3
The effect of substituent at the 7-, 8-, and 9-positions on benzene ring of different alloxazine and 5-deazaalloxazine analogs (**4**, **5** and **9**) docked into PTK

Compound	R^3 (**4**) or R (**5**, **9**)	ΔG_b (kcal/mol)	Inhibition constant (K_i)
4a	H	−8.03	1.29E−06
5a	H	−7.31	4.38E−06
4b	7-Me	−5.34	1.21E−04
5b	7-Me	−5.12	1.76E−04
4c	7-OMe	−4.66	3.86E−04
5c	7-OMe	−4.55	4.66E−04
4d	7-Cl	−5.30	1.31E−04
5d	7-Cl	−5.15	1.68E−04
4e	7-OH	−7.45	3.46E−06
5e	7-OH	−6.55	1.59E−05
4f	8-Me	−4.93	2.44E−04
5f	8-Me	−4.58	4.41E−04
4g	9-Me	−4.35	6.43E−04
5g	9-Me	−4.24	7.77E−04
4h	8-Cl	−5.39	1.13E−04
5h	8-Cl	−5.09	1.85E−04
4i	8-OH	−7.36	4.05E−06
5i	8-OH	−6.76	1.10E−05
4j	8-OMe	−4.97	2.26E−04
5j	8-OMe	−4.83	2.87E−04
4k	6,7,8-$(OMe)_3$	−2.54	0.01
5k	6,7,8-$(OMe)_3$	−2.48	0.02
4l	7-COOH	−3.99	0.00
9b	7-COOH	−3.97	0.00

Table 4
ΔG_b and K_i of pyridodipyrimidines (**11a–c**, **12**, **13a–f**, **14**, and **15**), bispyridodipyrimidines (**16** and **17a**, **b**) and pyrimidopteridines (**18a**, **b**, **19**, **20**, **21** and **22a–c**) docked into PTK

Compound	ΔG_b (kcal/mol)	Inhibition constant (K_i)
11a	−8.71	4.16E−07
11b	−8.01	1.35E−06
11c	−8.44	6.47E−07
12	−7.78	1.97E−06
13a	−1.70	0.06
13b	−1.89	0.04
13c	−6.19	2.89E−05
13d	−4.08	0.00
13e	+0.84	–[a]
13f	+0.93	–[a]
14	−4.02	0.00
15	−8.00	1.37E−06
16	+2.72	–[a]
17a	+1.58	–[a]
17b	+2.39	–[a]
18a	−2.50	0.01
18b	−8.39	7.11E−07
19	−2.91	0.01
20	−7.35	4.13E−06
21	−6.83	9.82E−06
22a	−7.65	2.48E−06
22b	−1.06	0.17
22c	−7.80	1.91E−06

[a] This cannot be calculated because ΔG_b is a positive value.

pyrimidopteridine, respectively, produced compounds having the best docking predicted affinities. Compounds containing H or Ph at the N-7 position and O or Ph at the C-8 position revealed the highest binding affinities. The lowest binding energies were obtained within the range of −6.19 to −8.71 kcal/mol as shown in Table 4. This favored docking affinity is attributed to the hydrophilic moieties, being three or four sets of imides, which act as hydrogen-acceptor (C═O) as well as hydrogen-donor (NH). These moieties enhance the hydrogen bond formation between the docked inhibitors and the target protein. As cited in literature [32], the compound with the higher number of hydrogen bonds, with the lowest binding energy, and with the smallest RMSD is generally said to be a reasonable candidate for the inhibition of the enzyme. In Table 4, we can notice that the majority of compounds with Ph ring at the 8 position such as **11a–c** and **15** have lower binding energies than their corresponding isomers with 8-oxo group. Compounds containing methyl group at the N-10 position such as **13a**, **b**, and **14**, at the N-3 position such as **13d**, or at both of N-3 and N-10 positions such as **13e**, **f** exhibited poor binding affinities, especially the last ones (**13e** and **f**, being of +0.84 and +0.93 kcal/mol, respectively). This reinforces the previous investigation for N-3 and N-10 substitutions, where compounds with methyl group at N-3 and/or N-10 positions, did not fit into the binding pocket of PTK.

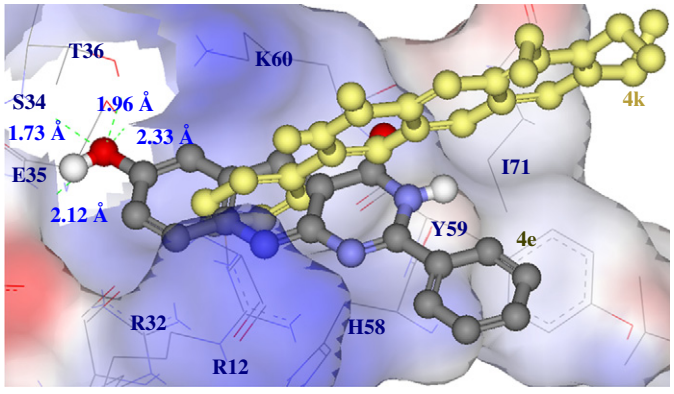

Fig. 5. The comparative binding interaction of 7-hydroxy (**4e**) and 6,7,8-trimethoxy (**4k**) derivatives of 2-deoxo-2-phenyl-5-deazaalloxazines docked into the binding site of PTK $pp60^{c\text{-}src}$. Compound **4e** (ΔG_b: −7.45 kcal/mol) is deeply fitted into the binding pocket showing four hydrogen bonds, whereas compound **4k** (ΔG_b: −2.54 kcal/mol) is improperly docked without any hydrogen bond.

The vertical-type bispyridodipyrimidines (**16**, with *n*-hexyl chain junction between its N-10 and N-10′ atoms) and the horizontal type (**17a**, **b**, with *n*-hexyl chain junction between their N-3 and N-3′ atoms), exhibited the poorest binding affinity into the binding site (Table 4). Owing to the bulkiness of the N10–N10′ and N3–N3′ bispyridodipyrimidines, and the methyl substitutions at N-3 and/or N-7 positions, the bispyridodipyrimidines showed high binding energies (ΔG_b) being +2.72 (**16**), +1.58 (**17a**), and +2.39 kcal/mol (**17b**). Consequently, they were rejected away from the binding pocket of PTK. Therefore, no hydrogen bond was detected between these bulky compounds and the target site. As shown in Fig. 6, compared with compound **16** (ΔG_b: +2.72 kcal/mol and RMSD: 14.60 Å), compound **7** has a good binding affinity (ΔG_b: −7.92 kcal/mol, RMSD: 2.25 Å) and exhibits one hydrogen bond between its *N*-oxide moiety and (NH) of Lys

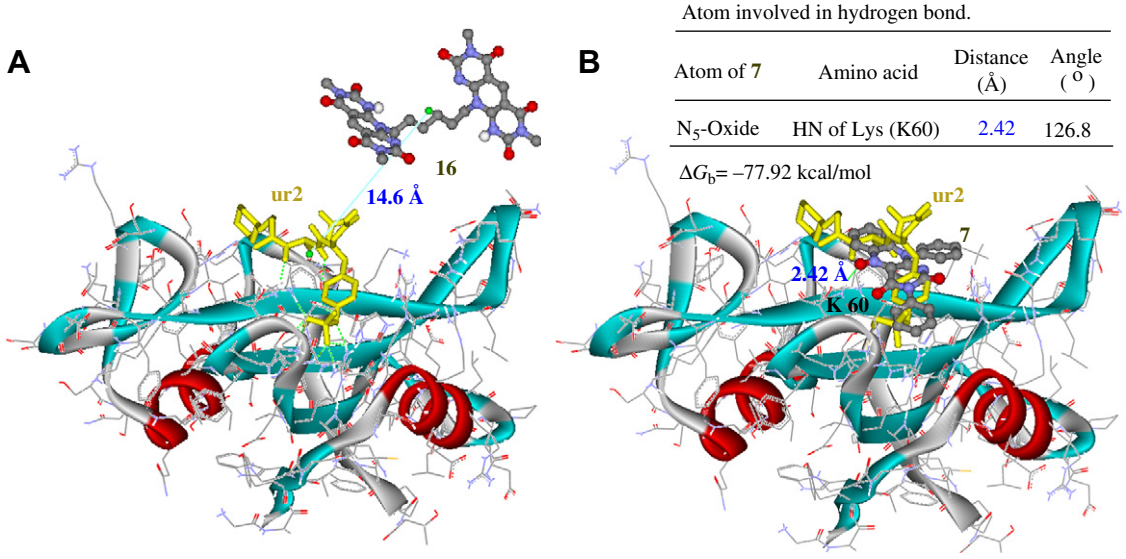

Fig. 6. The comparative binding affinities of **7** (3,10-diphenylflavin-5-oxide) and **16** (vertical-type bispyridodipyrimidine). (A) Compound **16** exhibited low binding affinity being ΔG_b: +2.72 kcal/mol with RMSD: 14.60 Å, without any hydrogen bond. (B) Compound **7** is superimposed onto the ur2 ligand being ΔG_b: −7.92 kcal/mol with RMSD: 2.25 Å, and exhibited one hydrogen bond with Lys 60.

60. We suggest the possibility in that the formation of hydrogen bond with the oxide anion of the flavin-5-oxides was responsible for increase in the activity of such type of derivatives [33].

2.9. Mode of interaction of the docked inhibitors into the protein tyrosine kinase (PTK)

The docked inhibitors oriented into the binding site similarly to the interaction of the native ur2 ligand into the Src SH2 domain of pp60$^{c\text{-}src}$ PTK 30]. Many compounds having a pyrimidin-4-one skeleton (i.e. compounds **2a**−**v** and **4a**−**r**) and a pyrimidine-2,4-dione skeleton (i.e. compounds **1a**−**s** and **3a**−**c**) fitted well into the hydrophilic domain of Arg 12, Arg 32, Ser 34, Glu 35, His 58, Tyr 59 and Lys 60 which is called pY (pTyr) pocket, where they bound into the target site with one to five hydrogen bonds. The hydrophobic domain of Cys 42, Ile 71, and Leu 94 residues encloses the non-polar moieties of the bound inhibitors, such as the 2-phenyl moiety of compounds **4b**, **e** or the 8-phenyl moiety of compound (**11b**). The docked inhibitors exhibited reasonable RMSD values in the range of 0.52−8.74 Å. On the other hand, compounds carrying more than two bulky phenyl rings were shown to shift slightly away from the hydrophilic domain. Therefore, they show none or a few hydrogen bonds into the binding site. For example, compound **11a** exerted the lowest binding energy (−8.71 kcal/mol) and smallest RMSD (0.52 Å), but owing to its four phenyl rings it was unable to form hydrogen bond within the binding site. As for the compounds containing *N*-10 phenyl moiety, such as **1l**, **11a**, and **18b**, their *N*-10 phenyl group is located perpendicularly to the phenyl ring of Tyr 59. While the imidazole ring of His 58 oriented by edge to the planar tricyclic moiety within a distance of 2.5−3.0 Å, and the facing angle of 109.4° as shown in Fig. 7 for compound **1l**, which exhibits one hydrogen bond with His 58 amino acid.

As cited in Table 5, the compounds of the best docking results with the lowest binding free energies are represented with their hydrogen bond interaction with the target macromolecule. These compounds include 2-deoxo-2,10-diphenyl-5-deazaflavin (**2i**) and the computationally designed 2-deoxo-2-phenyl-5-deazaalloxazines (**4a**), 2-deoxo-2-phenylflavin-5-oxides (**6a**, **b**), 3,10-diphenylflavin-5-oxide (**7**), pyridodipyrimidines, (**11b**, **c**, **12**, and **15**), and pyrimidopteridine (**22c**). They have 1−3 phenyl moieties, which are thought to be responsible for the planar aromatic fitting or electrostatic attraction onto the groove of the binding pocket. Also these properly docked compounds fulfill the structural features obtained by various SAR investigations' study as mentioned above. Regarding the hydrogen bond interaction according to Taylor et al. [34], they showed that C−H···O in crystals' contacts occur within certain distance (C···O, 3.0−4.0 Å) and angle ranges (C−H···O, 90−180°). The stronger the bond, the more linear it is likely to be [35]. Moreover, there is a general agreement in that for carbonyl acceptors, the H···O═C angle is distributed around 120°. Therefore, in our modeling results we consider the hydrogen bond angle greater than 110° to be of a reasonable strength.

We are encouraged to see that some of the computationally designed compounds such as **4a**, **6a**, **b**, **7**, **11b**, **c**, **12**, **15**, and **22c** showed good docking results suggesting that they are potentially active antitumor agents. These compounds comprise 1−3 phenyl moieties, which are thought to be responsible for the planar aromatic fitting or electrostatic attraction onto the groove of the binding pocket.

3. Conclusion

In this study, the biological activities of previously known 5-deazaflavins (**1a**−**s**), 2-deoxo-5-deazaflavins (**2a**−**d**, **j**), and 5-deazaalloxazine (**3a**−**c**) were investigated for their PKC

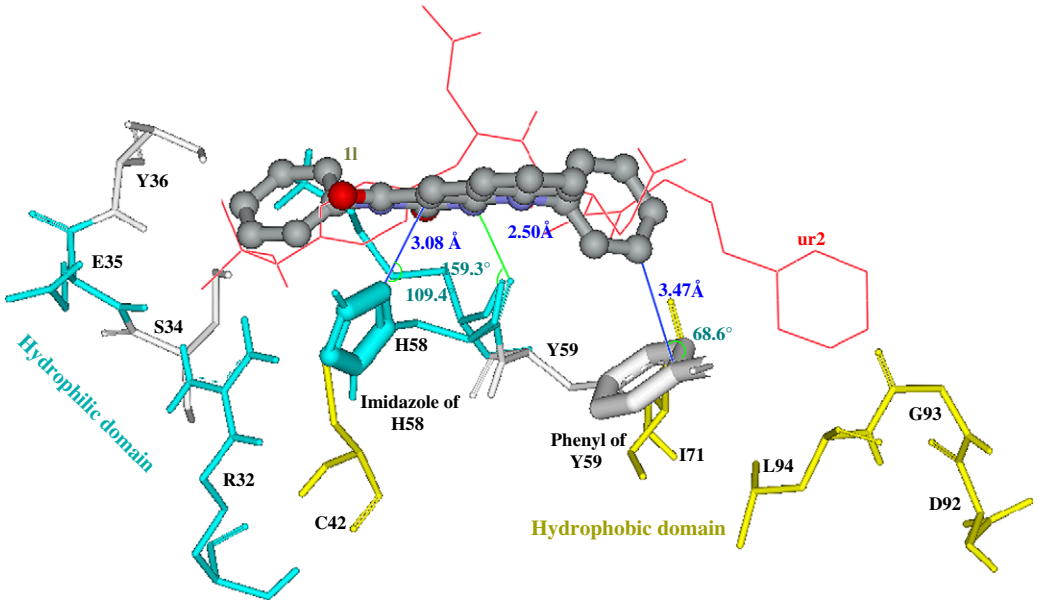

Fig. 7. Mode of interaction of compound **1l** (ball and stick, colored by element) docked into the binding site of PTK whose amino acids are shown as labeled sticks. It exhibited one hydrogen bond (shown in green line) with His 58. Both Arg 12 and Lys 60 amino acids are hidden for clearance. The hydrophilic domain, where the hydrogen bond was formed, is shown in cyan colored sticks. (For interpretation of the references to color in the text, the reader is referred to the web version of this article.)

and PTK inhibitory activities and cytotoxicities against *KB* tumor cells. The IC_{50} was correlated with their AutoDock binding free energies allowing us to design more potent PTK inhibitors. Interestingly, there was a good correlation between IC_{50} of the potential PTK active compounds (**1a**, **e**–**g**, **i**–**k** and **2a**, **b**, **d**, **j**) and their estimated AutoDock binding free energies (ΔG_b) with the correlation coefficient (R^2) of 0.593. The compounds, which exhibited the best docking results, are suggested to be potentially active including both the synthesized compound (**2i**) and the computationally designed structures (**4a**, **6a**, **b**, **7**, **11b**, **c**, **12**, **15**, and **22c**). The most effective inhibitory molecule group to the PTK with the highest binding affinity was elucidated by the following structural features: (1) 5-deazaflavins, flavins, and flavin-5-oxides having no substituent at the N-10 position (namely, alloaxazine type conformation) or Ph group at the N-10 position, (2), Ph or NH_2 group at the C-2 position, (3) hydrogen (or unsubstituted N-3), or Ph group at the N-3 position, (4) flavin-5-oxides as potentially more potent than the flavin and 5-deazaflavin analogs, and (5) pyridodipyrimidines and pyrimidopteridines which have H or Ph at the N-7 position and oxo or Ph at the C-8 position. The SAR of these compounds indicates that the phenyl moiety is necessary to produce good binding affinity either in C-2, N-3, N-7, C-8, or N-10 position. We have already confirmed this aspect by synthesis and in vitro and in vivo biological assay [4]. These phenyl moieties are involved in electrostatic surface attraction (van der Waals) into the binding pocket. Hydrogen bond interaction is commonly involved with the polar moieties, namely 4-oxo, 2-amino, N_3-H, N_5-oxide of flavin-5-oxides, and 6-oxo of pyridodipyrimidines and pyrimidopteridines. Moreover, horizontal and vertical-type bispyridodipyrimidines exhibited poor docking affinities in comparison with their monomers. The results of the docking study showed that 56 compounds with the above-mentioned structural features, out of 119 compounds, exhibited favorable binding free energies (−4.02 to −8.71kcal/mol), where the computationally designed compound **11c** was the best binder among all derivatives. The docked inhibitors behaved similar to the intact ur2 ligand into the binding pocket, exhibited up to five hydrogen bonds and showed reasonable to nearly reasonable RMSD values (0.52–8.74 Å). Compounds possessing more than two phenyl rings were shown to shift slightly from the binding site due to the steric hindrance. The phenyl moiety at the N10-position was shown to be oriented perpendicular to phenyl ring of Tyr 59 within the distance of 3–4 Å, while imidazole ring of His 58 was oriented by edge to the planar pyrimidoquinoline or benzopteridine nucleus within the distance of 2.5–5.0 Å.

4. Experimental protocols

4.1. Assay for protein kinase C (PKC)

The PKC assay developed by Oishi et al. [36] was used to determine the inhibitory effects of test compounds on PKC in vitro. The standard reaction mixtures contained appropriate amount of homogenous PKC (prepared from rat brain extracts), 25 μM of Tris/HCl (pH 7.5), 200 μM of $CaCl_2$, 5 μM of $MgCl_2$, PS (phosphatidylserine) at 25 μg/mL, histone III-S at 200 μg/mL and the dissolved compound was plated into each well of a 96-well plate. The reaction, started with the addition of the radioactive [γ-^{32}P] ATP (containing about 1×10^6 cpm), was carried out at 30 °C for 5 min. The reaction was stopped by the addition of TCA (trichloroacetic acid) solution. The reaction mixture was collected on a glass filter by

Table 5
The best docking results based on the binding free energies (ΔG_b) of compounds docked into PTK, the distance and angle of hydrogen bonds between compounds and amino acids involved in PTK, and RMSD from the crystallized ur2 ligand

Compound	ΔG_b (kcal/mol)	Hydrogen bonds between atoms of compound and amino acids				RMSD (Å)
		Atom of compound	Amino acid	Distance (Å)	Angle (°)	
11c	−8.44	N_9–N	HN of Arg 12	2.05	151.1	6.15
		C_6-Oxo	HN of Glu 35	1.91	152.5	
		C_6-Oxo	HN of Arg 32	2.04	156.2	
4a	−8.03	C_4-Oxo	HN of Glu 35	1.85	162.2	7.35
		C_4-Oxo	HN of Arg 32	1.73	159.3	
11b	−8.01	N_1–N	HN of Arg 32	2.22	150.0	3.74
		C_4-Oxo	HN of Lys 60	1.94	139.4	
		C_4-Oxo	HO of Ser 34	1.54	150.8	
		C_6-Oxo	HN of Lys 60	2.34	123.6	
15	−8.00	N_{10}–N	HN of His 58	1.91	168.2	5.53
7	−7.92	N_5-Oxide	HN of Lys 60	2.42	126.8	2.25
22c	−7.80	N_9–N	HN of Arg 12	2.17	140.1	8.29
12	−7.78	N_1–N	HN of Arg 12	2.20	148.6	7.44
		N_3–H	O of Glu 35	2.34	137.0	
		C_4-Oxo	HN of Glu 35	1.98	129.1	
		C_4-Oxo	HN of Thr 36	2.35	163.4	
		C_4-Oxo	HO of Ser 34	2.14	133.6	
2i	−7.77	N_1–N	HN of Arg 12	2.03	130.6	6.60
		C_4-Oxo	HN of Glu 35	2.07	159.7	
		C_4-Oxo	HN of Arg 32	1.80	163.9	
		C_4-Oxo	HN of Arg 32	2.43	136.5	
6b	−7.76	N_1–N	HN of Arg 12	2.00	154.4	8.01
		N_5-Oxide	HO of Ser 34	2.33	169.6	
		C_4-Oxo	HN of Arg 32	2.44	168.7	
		C_4-Oxo	HN of Thr 36	2.39	145.3	
		C_4-Oxo	HN of Glu 35	1.64	135.6	
6a	−7.67	N_1–N	HN of Arg 32	1.96	154.2	8.74
		C_4-Oxo	HN of Arg 32	1.38	130.9	
		N_5-Oxide	HS of Cys 42	1.70	157.8	

using a cell harvester, and specific radioactivity due to histone trapped on the filter was counted by a liquid scintillation counter. Radioactivity of samples containing the compounds relative to the control level was calculated, and 50% inhibitory concentrations (IC_{50}) were estimated.

*4.2. Growth inhibitory activities of 5-deazaflavins (**1a–l**) and 2-deoxo-2-phenyl-5-deazaflavins (**2a–d, j**) against human oral epidermoid carcinoma cell lines (KB)*

This assay was carried out by the modified standard MTT colorimetric assay [37] using [3-(4,5-dimethylthiazol-2-yl)-2,5-diphenyltetrazolium bromide, described previously in details [4]. The inhibitory effects of 5-deazaflavins (**1a–l**) and 2-deoxo-2-phenyl-5-deazaflavins (**2a–d**, **j**) were determined against KB (human oral epidermoid carcinoma) cell growth in vitro. The inhibition of cell growth (%) was calculated as $(1 - T/C) \times 100$, where C is the mean OD_{570} of the control group and T is that of the treated group. The IC_{50} was determined from the dose–response curve.

4.3. Preparation of target macromolecule

The target protein tyrosine kinases 1skj ($pp60^{c\text{-}src}$) was retrieved from the Protein Data Bank (http://www.rcsb.org/pdb/Welcome.do). All bound waters, ligands and cofactors were removed from the proteins. Kollman charges were computed using AutoDock 3.05. Polar hydrogen atoms were added subsequently. The amino acids of the binding site were defined using data in pdbsum (http://www.ebi.ac.uk/thornton-srv/databases/pdbsum/).

4.4. Compounds involved in this study

In this study, the potential protein tyrosine kinase binding activities were studied for 5-deazaflavins (**1a–s**) [2,3,17–19], 2-deoxo-5-deazaflavins (**2a–v**) [4,19,23,24], 5-deazaalloxazines (**3a–c**) [20–22], 2-deoxo-2-phenylflavin-5-oxides (**6c**) [4], 2-deoxo-2-phenylalloxazine (**9a**) [25], 5-alkylamino-5-deazaflavins (**10c–l**) [15], vertical- and horizontal-type bispyridodipyrimidines (**16** and **17a**, **b**) [27,28], and the computationally designed 2-deoxo-5-deazaalloxazins (**4a–r**), 3-phenylalloxazines (**5a–k**), 2-deoxo-2-phenylflavin-5-oxides (**6a**, **b**), 3,10-diphenylflavin-5-oxide (**7**), 2-deoxo-7,10-dimethyl-2-phenylflavin (**8**), 2-deoxo-2-phenylalloxazine (**9b**), 5-alkylamino-5-dezaflavins (**10a**, **b**), pyridodipyrimidines (**11–15**), and pyrimidopteridines (**18–22**).

4.5. Preparation of small molecule

ChemDraw 3D structures were constructed using ChemDraw 3D ultra 8.0 software [Molecular Modeling and Analysis;

Cambridge Soft Corporation, USA (2003)], and then they were energetically minimized by using MOPAC (semi-empirical quantum mechanics) with AM1 MOZYME geometry with 100 iterations and minimum RMS gradient of 0.10.

4.6. Protocol of molecular docking study using AutoDock 3.05

The grid encompassing the binding site, where the ligand was embedded, was created and the grid maps representing the co-crystallized ligand in the actual docking process were calculated using the AutoGrid (part of the AutoDock package). The grids (one for each atom type in the ligand plus one for electrostatic interactions) were chosen to be sufficiently large to include not only the active site but also significant portions of the surrounding surface. The size of the grid was thus $60 \times 60 \times 0$ in Å (angstrom) for the ur2 ligand with a grid spacing of 0.375 Å. Because the location of the original ligand in the complex was known, the cubic grids were centered on the ligand's binding site. Finally, AutoDock 3.05 was run to calculate the binding free energy of a given ligand conformation in the crystal structure. The probable inaccuracies of structures were ignored in the calculations. Of the three different search algorithms offered by AutoDock 3.05, the genetic algorithm with local search (GALS) was applied to the model for the interaction/binding between the target macromolecule and the docked ligand. For the local search, the so-called pseudo-Solis and Wets algorithm was used. The 250 independent docking runs were performed for each docking case. Cluster analysis was performed on the docked results using a root mean square (RMS) tolerance of 0.5 Å. The clusters were ranked from the averaged lowest energy obtained for members to the highest. The analysis was carried out for the top 10 docking clusters. The mode of interaction of the ur2 within 1skj was used as a standard docked model as well as for RMSD calculation. All calculations were carried out on Linux based machine. The inhibitors were compared according to the best binding free energy (minimum) obtained among all the runs.

4.7. Molecular modeling and analysis of the binding mode

To select the most probable conformation of the complexes given by AutoDock, we applied quantitative and qualitative considerations. First, we chose the conformation with the lowest final docked energy as the starting point. Then the chosen conformation was analyzed qualitatively based on the location/orientation of the inhibitor in relation to the intact ligand (ur2). Therefore, if the docked inhibitor was not in accordance with the location/orientation of the intact bound ur2 ligand, the docked complex was discarded and the next docked conformation was analyzed. This procedure was repeated until we found a conformation in good harmony with the corresponding ur2 ligand as the binding model. Each of the clusters, that exhibited significant negative interaction energies, was examined by using Accelrys Discovery Studio version 1.6 [Accelrys, Inc., San Diego, CA, USA (2006)] for the molecular modeling investigation. It was used for evaluation of the mode of interaction, measurement of RMSD, and evaluation of hydrogen bonds in ligand–receptor interaction.

Acknowledgements

This work was supported by Research Grant of Taisho Pharmaceutical Co., Ltd, Saitama, Japan. This was also supported by Collaborative Research Grant A of Kobe Gakuin University, Japan. The authors are indebted to the SC-NMR Laboratory of Okayama University for the NMR spectral measurements and the Okayama University Information Technology Center for using Accelrys Discovery Studio 1.6. The authors are grateful to each organization for their generous support for our current work.

References

[1] T. Nagamatsu, F. Yoneda, Y. Kawashima, T. Yamagishi, H. Ikeya, The Sixth Annual Meeting of Division of Medicinal Chemistry, Book Abstract, Tsukuba, Japan, 1987, pp. 148–149.
[2] T. Nagamatsu, Y. Hashigushi, F. Yoneda, J. Chem. Soc., Perkin Trans. 1 (1984) 561–565.
[3] T. Nagamatsu, K. Kuroda, N. Mimura, R. Yanada, F. Yoneda, J. Chem. Soc., Perkin Trans. 1 (1994) 1125–1128.
[4] H.I. Ali, K. Tomita, E. Akaho, H. Kambara, S. Miura, H. Hayakawa, N. Ashida, Y. Kawashima, T. Yamagishi, H. Ikeya, F. Yoneda, T. Nagamatsu, Bioorg. Med. Chem. 15 (2007) 242–256.
[5] F. Hollósy, G. Keri, Curr. Med. Chem. Anticancer Agents 4 (2004) 173–197.
[6] O.V. Buzko, A.C. Bishop, K.M. Shokat, J. Comput. Aided Mol. Des. 16 (2002) 113–127.
[7] M. Kontoyianni, L.M. McClellan, G.S. Sokol, J. Med. Chem. 47 (2004) 558–565.
[8] T.J.A. Ewing, S. Makino, A.G. Skillman, I.D. Kuntz, J. Comput. Aided Mol. Des. 15 (2001) 411–428.
[9] G.M. Morris, D.S. Doodsell, R.S. Holliday, R. Huey, W.E. Hart, R.K. Belew, A.J. Olson, J. Comput. Chem. 19 (1998) 1639–1662.
[10] Z. Hu, S. Wang, W.M. Southerland, ACS Division of Chemical Information Final Program, 228th ACS National Meeting, Philadelphia, PA, August 2004, pp. 22–26.
[11] R. Wang, Y. Lu, S. Wang, J. Med. Chem. 46 (2003) 2287–2303.
[12] R.C. Jackson, Curr. Opin. Biotechnol. 6 (1995) 646–651.
[13] D.E. O'Brien, L.T. Weinstock, C.C. Cheng, J. Heterocycl. Chem. 7 (1970) 99–105.
[14] J.M. Wilson, G. Henderson, F. Black, A. Sutherland, R.L. Ludwig, K.H. Vousden, D.J. Robins, Bioorg. Med. Chem. 15 (2007) 77–86.
[15] T. Kimachi, F. Yoneda, T. Sasaki, J. Heterocycl. Chem. 29 (1992) 763–765.
[16] C. Chug, R.L. Geahlen, J. Nat. Prod. 55 (1992) 1529–1560.
[17] F. Yoneda, Y. Sakuma, S. Mizumoto, R. Ito, J. Chem. Soc., Perkin Trans. 1 (1976) 1805–1808.
[18] F. Yoneda, K. Tsukuda, K. Shinozuka, F. Hirayama, K. Uekama, A. Koshiro, Chem. Pharm. Bull. 28 (1980) 3049–3056.
[19] F. Yoneda, K. Mori, M. Ono, Y. Kadokawa, E. Nagao, H. Yamaguchi, Chem. Pharm. Bull. 28 (1980) 3514–3520.
[20] O.A. Sayed, F.M. El-Bieh, S.I. El-Aqeel, B.A. Al-Bassam, M.E. Hussein, R.U. Roy, K.R. Desai, Indian J. Heterocycl. Chem. 14 (2005) 327–330.
[21] F. Yoneda, F. Takayama, A. Koshiro, Chem. Pharm. Bull. 27 (1979) 2507–2510.

[22] W. Pfleiderer, F. Sagi, L. Grozinger, Chem. Ber. 99 (1966) 3530–3538.
[23] H.I. Ali, A. Noriyuki, T. Nagamatsu, Bioorg. Med. Chem., accepted for publication.
[24] T. Aoyagi, R. Yanada, K. Bessho, F. Yoneda, W.L.F. Armarego, J. Heterocycl. Chem. 28 (1991) 1537–1539.
[25] F. Yoneda, S. Matsumoto, Y. Sakuma, J. Chem. Soc., Perkin Trans. 1 (1975) 1907–1909.
[26] E. Akaho, G. Morris, D. Goodsell, D. Wong, A. Alson, J. Chem. Software 7 (2001) 103–114.
[27] H. Yamato, T. Nagamatsu, F. Yoneda, J. Heterocycl. Chem. 28 (1991) 1209–1211.
[28] F. Yoneda, K. Tanaka, H. Yamato, K. Moriyama, T. Nagamatsu, J. Am. Chem. Soc. 111 (1989) 9199–9202.
[29] Y. Sakuma, S. Matsumoto, T. Nagamatsu, F. Yoneda, Chem. Pharm. Bull. 24 (1976) 338–341.
[30] T. Nagamatsu, H. Yamato, M. Ono, S. Takarada, F. Yoneda, J. Chem. Soc., Perkin Trans. 1 (1992) 2101–2109.
[31] M.S. Plummer, D.R. Holland, A. Shahripour, E.A. Lunney, J.H. Fergus, J.S. Marks, P. McConnell, W.T. Mueller, T.K. Sawyer, J. Med. Chem. 40 (1997) 3719–3725.
[32] E. Akaho, C. Fujikawa, H.I. Runion, C.R. Hill, H. Nakaho, J. Chem. Software 5 (1999) 147–162.
[33] N. Haginoya, S. Kobayashi, S. Komoriya, T. Yoshino, T. Nagata, Y. Hirokawa, T. Nagahara, Bioorg. Med. Chem. 12 (2004) 5579–5586.
[34] R. Taylor, O. Kennard, J. Am. Chem. Soc. 104 (1982) 5063–5070.
[35] R. Taylor, O. Kennard, Acc. Chem. Res. 17 (1984) 320–326.
[36] K. Oishi, R.L. Raynor, P.A. Charp, J.F. Kuo, J. Biol. Chem. 263 (1988) 6865–6871.
[37] S. Miura, Y. Yoshimura, M. Endo, H. Machida, A. Matsuda, M. Tanaka, T. Sasaki, Cancer Lett. 129 (1998) 103–110.